Unified explanation of $b \to s\mu^+\mu^-$ anomalies, neutrino masses, and $B \to \pi K$ puzzle

Alakabha Datta[*] and John Waite[†]

*Department of Physics and Astronomy, 108 Lewis Hall,
University of Mississippi, Oxford, Mississippi 38677-1848, USA*

Divya Sachdeva[‡]

Department of Physics and Astrophysics, University of Delhi, Delhi 110 007, India

Anomalies in semileptonic B decays could indicate new physics beyond the standard model (SM). There is an older puzzle in nonleptonic $B \to \pi K$ decays. The new particles, leptoquarks and diquarks, required to solve the semileptonic and the nonleptonic puzzles can also generate neutrino masses and mixing at loop level. We show that a consistent framework to explain the B anomalies and the neutrino masses is possible and we make predictions for certain rare nonleptonic B decays.

I. INTRODUCTION

Searching for beyond the SM (BSM) physics has been the primary focus of the high energy community. Rare B decays have been widely studied to look for BSM effects. Because these decays get small SM contributions, new physics (NP) can compete with the SM and produce deviations from SM predictions. Over the last few years measurements in certain B decays have shown deviations from the SM. These deviations are observed in two groups—in charged current (CC) processes mediated by the $b \to c\tau^-\bar{\nu}$ tansitions and in the neutral current (NC) processes mediated by $b \to s\ell^+\ell^-$ transition with $\ell = \mu, e$. We will focus here on the NC anomalies although it is possible that the CC and the NC anomalies are related [1] but we will not explore that possibility here.

Let us start with the $b \to s\ell^+\ell^-$ decays which are fertile grounds to look for new physics effects [2,3]. In $b \to s\mu^+\mu^-$ transitions there are discrepancies with the SM in a number of observables in $B \to K^*\mu^+\mu^-$ [4–8] and $B_s^0 \to \phi\mu^+\mu^-$ [9,10].

There are also measurements that are different from the SM expectations that involve ratios of $b \to s\mu^+\mu^-$ and $b \to se^+e^-$ transitions. These measured quantities are tests of lepton universality violation (LUV) and are defined as $R_K \equiv \mathcal{B}(B^+ \to K^+\mu^+\mu^-)/\mathcal{B}(B^+ \to K^+e^+e^-)$ [11,12] and $R_{K^*} \equiv \mathcal{B}(B^0 \to K^{*0}\mu^+\mu^-)/\mathcal{B}(B^0 \to K^{*0}e^+e^-)$ [13,14].

While the discrepancies in $b \to s\mu^+\mu^-$ can be understood with lepton universal new physics [15], hints of LUV in R_K and R_K^* require NP that couple differently to the lepton generations. A well-studied scenario is to assume NP coupling dominantly to the muons though NP coupling to electrons is not ruled out [16,17]. The $b \to s\mu^+\mu^-$ transitions are defined via an effective Hamiltonian with vector and axial vector operators:

$$H_{\text{eff}} = -\frac{\alpha G_F}{\sqrt{2}\pi}V_{tb}V_{ts*}\sum_{a=9,10}(C_aO_a + C'_aO'_a),$$

$$O_{9(10)} = [\bar{s}\gamma_\mu P_L b][\bar{\mu}\gamma^\mu(\gamma_5)\mu], \tag{1}$$

where the V_{ij} are elements of the Cabibbo-Kobayashi-Maskawa (CKM) matrix and the primed operators are obtained by replacing L with R. It is assumed Wilson coefficients (WCs) include both the SM and NP contributions: $C_X = C_{X,\text{SM}} + C_{X,\text{NP}}$. One now fits to the data to extract $C_{X,\text{NP}}$. There are several scenarios that give a good fit to the data and results of recent fits can be found in Ref. [17–22]. One popular scenario is $C_{9,\text{NP}}^{\mu\mu} = -C_{10,\text{NP}}^{\mu\mu}$ which can arise from the tree-level exchange of leptoquarks (LQ) or a Z' which may be heavy [23–26] or light [16,27–31]. Here we will focus on the LQ solution and there are three types of LQ that can generate this scenario. These are the $SU(2)_L$-triplet scalar (S_3), the $SU(2)_L$-singlet vector (U_1), and the $SU(2)_L$-triplet vector (U_3). We will focus on the S_3 which along with diquarks can be used to generate neutrino masses at loop level [32,33]. To generate the

[*]datta@phy.olemiss.edu
[†]jvwaite@go.olemiss.edu
[‡]divyasachdeva951@gmail.com

neutrino masses, one can fix the S_3 couplings by a fit to the $b \to s\ell^+\ell^-$ data and then the diquark couplings are constrained from the neutrino parameters. In this paper we point out that the diquark couplings can be fixed from nonleptonic B decays and now one can check whether the correct neutrino masses and mixings are reproduced. We would like to mention that joint explanation of $R_K^{(*)}$ and $R_D^{(*)}$ was first pointed out in [1] and later a connection between $R_K^{(*)}$ or $R_D^{(*)}$ and neutrino masses was discussed in [34–36]. Here, we are anticipating a common framework with leptoquarks and diquarks that can explain the semileptonic and nonleptonic B measurements along with the neutrino masses and mixing.

The observations that we will use for the nonleptonic decays are the set of $B \to \pi K$ decays. These are penguin dominated nonleptonic b decays and have been studied extensively. The decays in the set include $B^+ \to \pi^+ K^0$ (designated as +0), $B^+ \to \pi^0 K^+$ (0+), $B^0 \to \pi^- K^+$ (−+), and $B^0 \to \pi^0 K^0$ (00). Their amplitudes are not independent, but obey a quadrilateral isospin relation:

$$\sqrt{2}A^{00} + A^{-+} = \sqrt{2}A^{0+} + A^{+0}. \tag{2}$$

Using these decays, nine observables have been measured: the four branching ratios, the four direct CP asymmetries A_{CP}, and the mixing-induced indirect CP asymmetry S_{CP} in $B^0 \to \pi^0 K^0$. Shortly after these measurements were first made (in the early 2000s), it was noted that there was an inconsistency among them. This was referred to as the "$B \to \pi K$ puzzle" [37–40].

Recently the fits were updated [41–43]. In Ref. [41] it was observed that the key input to understanding the data was the ratio of the color-suppressed tree amplitude (C') to the color-allowed (T') amplitude. Theoretically, this ratio is predicted to be $0.15 \lesssim |C'/T'| \lesssim 0.5$ [44] with a default value of around 0.2. It was found that for a large $|C'/T'| = 0.5$, the SM can explain the data satisfactorily. However, with a small, $|C'/T'| = 0.2$, the fit to the data has a p value of 4%, which is poor. Hence, if $|C'/T'|$ is small, the SM cannot explain the $B \to \pi K$ puzzle—NP is needed. The precise statement of the situation is then, the measurements of $B \to \pi K$ decays *allow* for NP and so in this paper we will assume there is NP in these decays. There are two types of NP mediators that one can consider for the $B \to \pi K$ decays. One is a Z' boson that has a flavor-changing coupling to $\bar{s}b$ and also couples to $\bar{u}u$ and/or $\bar{d}d$. The second option is a diquark that has db and ds couplings or ub and us couplings. We will focus on the diquark explanation as the diquarks can contribute to neutrino masses.

The paper is organized in the following manner. In Sec. II we describe the setup with leptoquarks and diquarks that leads to neutrino masses and mixing at the loop level. In that section we also discuss the low energy constraints

for the leptoquark Yukawa couplings including the $b \to s\ell^+\ell^-$ data. In Sec. III we explore the $B \to \pi K$ decays mediated by the exchange of diquarks and we consider the constraints on the diquark Yukawa couplings from the $B \to \pi K$ decays and meson oscillations. In Sec. IV we consider the collider constraints on the diquark and leptoquarks coupling and masses and we give a scan of all their couplings that satisfy all the constraints and generate the correct neutrino masses and couplings. For a few benchmark cases we present explicit expressions for the diquark and the leptoquark Yukawa couplings and predict the branching ratios for the rare decays $B \to \phi\pi$ and $B \to \phi\phi$. Finally in Sec. V we present our conclusions.

II. COLORED ZEE BABU MODEL

We briefly summarize the main features of the colored Zee Babu model [32,45] that are central to our idea. The model includes a scalar leptoquark S_{3L} (with lepton number 1) of mass m_L and a scalar diquark S_D of mass m_S transforming as[1] $(3, 3, -1/3)$ and[2] $(6, 1, -2/3)$ respectively under SM gauge group $SU(3)_c \times SU(2) \times U(1)_Y$ with $Q = T_3 + Y$. The baryon number of S_{3L} is taken to be $1/3$ whereas S_D is assigned $2/3$. With this assignment of baryon number, the baryon conservation is automatic and thus the proton decay is forbidden. The lepton number is softly broken through a trilinear term thereby generating Majorana neutrino mass.

With the particle content discussed above, the interaction Lagrangian is given as

$$\mathcal{L}_{\text{int}} = -Y_l^{ij}\overline{L_i^c}i\sigma_2 Q_j^\alpha S_{3L}^{\alpha*} - Y_d^{ij}\overline{d_{iR}^{\alpha c}}d_{jR}^\beta S_D^{\alpha\beta*}$$
$$+ \mu S_{3L}^{\alpha*}S_{3L}^{\beta*}S_D^{\alpha\beta} + \text{H.c.}, \tag{3}$$

where $\alpha, \beta = r, b, g$ are $SU(3)_c$ indices, $i, j = 1, 2, 3$ are generation indices, the diquark coupling matrix, Y_d^{ij}, is a symmetric complex matrix whereas the leptoquark coupling matrix, Y_l^{ij}, is a general complex matrix. The leptoquark couples to leptons and quarks as $\sqrt{2}\nu_{iL}u_{jL} - \sqrt{2}e_{iL}d_{jL} + \nu_{iL}d_{jL} + e_{iL}u_{jl}$. Note that, in Eq. (3), we can also have additional scalar interaction terms (not relevant to our analysis), such as

$$\lambda_1 \Phi^\dagger \Phi \text{Tr}(S_{3L}^\dagger S_{3L}) + \lambda_2 \text{Tr}(\Phi^\dagger S_{3L} S_{3L}^\dagger \Phi)$$

where Φ is a Higgs doublet. These terms give rise to splitting in the mass of S_{3L} particles, comprising three states of different electric charges $-4/3$, $-1/3$, and $2/3$, and thus

---

[1]The choice $(3, 1, -1/3)$ is also possible as it couples neutrinos to down-type quarks but will not explain the R_K and R_K^* anomaly as this scalar couples up-type quarks to charged leptons.

[2]Note that if we had chosen the diquark to be $(3, 1, -2/3)$, Y_d and, hence, the neutrino mass matrix would be antisymmetric.
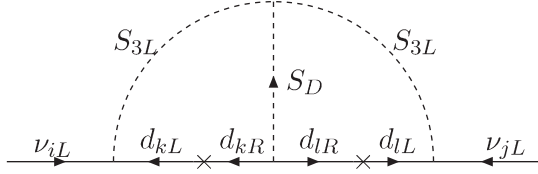
FIG. 1. The two loop neutrino mass generated by $(3, 3, -1/3)$ leptoquark and $(6, 1, -2/3)$ diquark.

contribute to the oblique corrections [46]. To avoid that, we assume $\lambda_{1,2} = 0$ such that all S_{3L} particles/states have same mass, m_L. Along with this, there are quartic and quadratic terms of these scalars. We assume that their coefficients are adjusted such that only the Higgs doublet gets the vev and the potential is bounded from below.

The above Lagrangian can generate majorana neutrino mass at two loop as depicted in the Fig. 1. The resultant neutrino matrix is given as [32,47]

$$M_\nu^{ij} = 24\mu Y_l^{ik} m_d^{kl} Y_d^{lm} I^{lm} m_d^{mn} Y_l^{nj}, \quad (4)$$

where I^{kl} is a loop integral, which in the limit of large leptoquark and diquark masses simplifies to

$$I^{kl} \simeq \frac{1}{(4\pi)^4} \frac{1}{m_L^2} \tilde{I}\left(\frac{m_S^2}{m_L^2}\right), \quad (5)$$

with

$$\tilde{I}(r) = \int_0^1 dx \int_0^{1-x} dy \frac{1}{x+y(y+r-1)} \ln\left(\frac{x+ry}{y(1-y)}\right), \quad (6)$$

and m_d is 3×3 diagonal mass matrix for down-type quarks. Note that we have chosen diagonal bases of the mass matrix for down-type quarks and charged leptons. Hence, to obtain the correct masses of neutrino, we need to diagonalize the mass matrix, M_ν by the Pontecorvo-Maki-Nakagawa-Sakata matrix $\mathcal{U}$ as

$$m_\nu = \mathcal{U}^\dagger M_\nu \mathcal{U}. \quad (7)$$

The standard parametrization is adopted such that

$$\mathcal{U} = \begin{pmatrix} 1 & 0 & 0 \\ 0 & c_{23} & s_{23} \\ 0 & -s_{23} & c_{23} \end{pmatrix} \begin{pmatrix} c_{13} & 0 & s_{13}e^{-i\delta} \\ 0 & 1 & 0 \\ -s_{13}e^{i\delta} & 0 & c_{13} \end{pmatrix}$$

$$\times \begin{pmatrix} c_{12} & s_{12} & 0 \\ -s_{12} & c_{12} & 0 \\ 0 & 0 & 1 \end{pmatrix} \begin{pmatrix} 1 & 0 & 0 \\ 0 & e^{i\alpha_{21}/2} & 0 \\ 0 & 0 & e^{i\alpha_{31}/2} \end{pmatrix} \quad (8)$$

where c_{ij} and s_{ij} represent $\cos\theta_{ij}$ and $\sin\theta_{ij}$, respectively. In the case of Majorana neutrinos, α_{21} and α_{31} are the extra

CP phases that cannot be determined by the oscillation experiments. However, these phases could be sensitive to the upcoming neutrinoless double beta decay searches.

It should be noted that the mass dimension one parameter, μ, is constrained by demanding the perturbativity of the theory. The trilinear term in the Eq. (3) generates one-loop corrections to leptoquark and diquark masses. These corrections (Δm^2) are, in general, proportional to $\frac{\mu^2}{16\pi^2}$. Requiring corrections to be smaller than the corresponding masses implies $\mu \ll 4\pi m_{S/L}$ [47]. As various collider searches, discussed in Sec. V, do not allow the scalar masses to be smaller than 1 TeV, we take μ from 0.1 to 1 TeV and this choice commensurates with the above constraints.

Having discussed the details of the model, next we list all the possible constraints, coming from various experiments on leptoquark and diquark coupling matrices.

III. LEPTOQUARKS

A. Lepton flavor violation at tree level

Collider searches of leptoquarks indicate that they are heavy. So we can study their low energy effects by writing 4-Fermi operators of two lepton-two quarks. Using Fierz rearrangement, we get

$$\frac{Y_l^{ik} Y_l^{jn*}}{2m_L^2} (\bar{l}_i \gamma^\mu P_L l_j)(\bar{q}_k \gamma_\mu P_L q_n) + \text{H.c.}$$

as an effective operator where l and q denote leptons and quarks. These are organized in terms of the four-Fermi effective interactions with normalized dimensionless Wilson coefficients as

$$\mathcal{H}_{\text{eff}} = \sum_{ijkn} \frac{Y_l^{ik} Y_l^{jn*}}{2m_L^2} \mathcal{O}_{ijkn} = \frac{-4G_F}{\sqrt{2}} \sum_{ijkn} C^{ijkn} \mathcal{O}_{ijkn}.$$

In Ref. [48], constraints on such operators have been extensively studied. Keeping in mind that Y_l^{ij} should be able to explain a small neutrino mass, following are the most crucial operators related to our work:

(1) $(\overline{e_i}\gamma^\mu P_L e_j)(\bar{d}\gamma_\mu P_L d)$: The μ-e conversion in nuclei sets a bound on the Wilson coefficient of this operator, i.e.,

$$C^{1211} = \left|\frac{Y_l^{11} Y_l^{21*}}{4\sqrt{2}G_F m_L^2}\right| < 8.5 \times 10^{-7}. \quad (9)$$

(2) $(\bar{\mu}\gamma^\mu P_L e)(\bar{d}\gamma_\mu P_L s)$: The bound from the decay $K^\circ \to e^+\mu^-$ sets a bound on C^{1212}

$$C^{1212} = \left|\frac{Y_l^{12} Y_l^{21*}}{4\sqrt{2}G_F m_L^2}\right| < 3.0 \times 10^{-7}. \quad (10)$$

(3) $(\overline{\nu_i}\gamma^\mu P_L \nu_j)(\overline{d_k}\gamma_\mu P_L d_l)$: The constraint on the K meson decay to pion and neutrinos $(\nu_i \nu_j)$ sets another bound:

$$C^{ij12} = \left| \frac{Y_l^{i1} Y_l^{j2*}}{4\sqrt{2} G_F m_L^2} \right| < 9.4 \times 10^{-6}. \quad (11)$$

Apart from this, we have also taken care of all the relevant Wilson coefficients mentioned in Ref. [48].

B. Lepton flavor violation radiative decay

The lepton flavor violation radiative decays $l_i \to l_j \gamma$ are induced at one loop by the exchange of a leptoquark S_{3L} with the branching ratio [46]

$$\text{BR}(\ell_i \to \ell_j \gamma) \simeq \frac{3\alpha\chi_i}{256\pi G_F^2} \frac{1}{m_L^4} |(Y_l Y_l^\dagger)^{ij}|^2 \quad (12)$$

where $\alpha = \frac{e^2}{4\pi}$, $\chi_\mu = 1$, and $\chi_\tau = 1/5$. In the case of a τ lepton, there are two leptonic modes and hadronic modes can be approximated by a single partonic mode (with three colors). Hence there is a factor of 5 difference in μ and the τ-lepton branching ratio. The current experimental bounds [49,50] are
(1) $\text{BR}(\mu \to e\gamma) < 4.2 \times 10^{-13}$,
(2) $\text{BR}(\tau \to \mu\gamma) < 4.4 \times 10^{-8}$,
(3) $\text{BR}(\tau \to e\gamma) < 3.3 \times 10^{-8}$.

C. $b \to s\ell^+\ell^-$ anomalies

As discussed in the Introduction one can perform fits to the $b \to s\ell^+\ell^-$ data and scenarios in terms of Wilson's coefficients that give a good description of the data. In the above set up, the exchange of the S_{3L} leptoquark at tree level contributes to the decay $b \to s\ell^+\ell^-$, and in particular generates the scenario $C_{9,\text{NP}}^{\mu\mu} = -C_{10,\text{NP}}^{\mu\mu}$. The effective Hamiltonian describing the decay is parametrized as

$$\mathcal{H}_{\text{eff}} = -\frac{4G_F}{\sqrt{2}} \frac{\alpha}{4\pi} V_{tb} V_{ts*} \sum_i C_i(\mu) \mathcal{O}_i(\mu) + \text{H.c.}, \quad (13)$$

where $\mathcal{O}_i(\mu)$ are effective operators with Wilson coefficients $C_i(\mu)$ renormalized at the scale μ. For the model under consideration, only the operators $\mathcal{O}_9^{\ell_i} = (\bar{s}\gamma^\mu P_L b)(\bar{\ell}_i \gamma^\mu \ell_i)$ and $\mathcal{O}_{10}^{\ell_i} = (\bar{s}\gamma^\mu P_L b)(\bar{\ell}_i \gamma^\mu \gamma_5 \ell_i)$ are induced. Using Fierz identity, we obtain the following Wilson coefficients:

$$C_9^{\ell_i} = -C_{10}^{\ell_i} = -\frac{\sqrt{2}\pi}{4\alpha G_F m_L^2} \frac{(Y_l^{i3})(Y_l^{i2*})}{V_{tb} V_{ts*}}. \quad (14)$$

Assuming new physics only in the muon sector, a model independent analysis on the above operators [17] from the R_K, R_K^*, P_5' and other observables suggests that

$$C_9^{\mu\mu}(\text{NP}) = -0.53 \pm 0.08.$$

IV. DIQUARK

A. Nonleptonic decays and the $B \to \pi K$ puzzle

In the Standard Model the amplitudes for hadronic B decays of the type $b \to q\bar{f}f$ are generated by the following effective Hamiltonian:

$$H_{\text{eff}}^q = \frac{G_F}{\sqrt{2}} \left[V_{fb} V_{fq}^* (c_1 O_{1f}^q + c_2 O_{2f}^q) - \sum_{i=3}^{10} V_{tb} V_{tq}^* c_i^t O_i^q \right] + \text{H.c.}, \quad (15)$$

where the superscript t indicates the internal quark, and f can be a u or c quark. q can be either a d or an s quark depending on whether the decay is a $\Delta S = 0$ or $\Delta S = -1$ process. The operators O_i^q are defined as

$$O_{f1}^q = \bar{q}_\alpha \gamma_\mu L f_\beta \bar{f}_\beta \gamma^\mu L b_\alpha, \quad O_{2f}^q = \bar{q}\gamma_\mu L f \bar{f}\gamma^\mu L b,$$
$$O_{3,5}^q = \bar{q}\gamma_\mu L b \bar{q}'\gamma^\mu L(R) q', \quad O_{4,6}^q = \bar{q}_\alpha \gamma_\mu L b_\beta \bar{q}'_\beta \gamma^\mu L(R) q'_\alpha,$$
$$O_{7,9}^q = \frac{3}{2}\bar{q}\gamma_\mu L b e_{q'} \bar{q}'\gamma^\mu R(L) q',$$
$$O_{8,10}^q = \frac{3}{2}\bar{q}_\alpha \gamma_\mu L b_\beta e_{q'} \bar{q}'_\beta \gamma^\mu R(L) q'_\alpha, \quad (16)$$

where $R(L) = 1 \pm \gamma_5$, and q' is summed over u, d, s, c, and b. O_2 and O_1 are the tree-level and QCD corrected operators, respectively. O_{3-6} are the strong gluon induced penguin operators, and operators O_{7-10} are due to γ and Z exchange (electroweak penguins) and "box" diagrams at loop level. The Wilson coefficients c_i^f are defined at the scale $\mu \approx m_b$ and have been evaluated to next-to-leading order in QCD. The c_i^t are the regularization scheme independent values and can be found in Ref. [44].

The diquarks discussed in Sec. II in the context of neutrino mass generation can contribute to the $B \to \pi K$ decays and we can write down the new physics operators that will be generated by a 6 or $\bar{3}$ diquark [51]. In the general case we get the effective Hamiltonian for b quark decays $b \to \bar{d}_i d_j d_k$ as

$$\mathcal{H}_{\text{NP}}^d = X^d \bar{d}_{\alpha,k} \gamma_\mu (1 + \gamma^5) b_\alpha \bar{d}_{\beta,j} \gamma^\mu (1 + \gamma^5) d_{\beta,i}, \quad (17)$$

where the superscript d in X^d equals 6 or $\bar{3}$ corresponding to the color sextet or the antitriplet diquark. The greek subscripts represent color and the latin subscripts the flavor. We have

$$X^d = -\frac{Y_{i3}^d Y_{jk}^{*d}}{4m_S^2}, \quad (18)$$

where the Yukawa Y are symmetric for the sextet diquark and antisymmetric for the antitriplet diquark and we have assumed the same masses for the diquarks.

For b decays of the type $b \to \bar{s}ss$ the diquark contribution is tiny as the effective Hamiltonian is proportional to Y_{22}^d which vanishes for the $\bar{3}$ diquark and is highly suppressed from K and B mixing for the sextet diquark. Similarly the $b \to \bar{d}dd$ transition is proportional to Y_{11}^d, which is also small.

For $b \to s\bar{d}d$ ($b \to \bar{d}sd$ and $b \to \bar{d}ds$) transitions we have the following Hamiltonian:

$$\mathcal{H}_{\mathrm{NP}}^d = X^d \bar{s}_\alpha \gamma_\mu (1+\gamma^5) b_\alpha \bar{d}_\beta \gamma^\mu (1+\gamma^5) d_\beta$$
$$+ X_C^d \bar{s}_\alpha \gamma_\mu (1+\gamma^5) b_\beta \bar{d}_\beta \gamma^\mu (1+\gamma^5) d_\alpha, \quad (19)$$

with

$$X^d = -\frac{Y_{13}^d Y_{12}^{*d}}{4m_S^2},$$

$$X_C^d = -\frac{Y_{13}^d Y_{21}^{*d}}{4m_S^2}, \quad (20)$$

and

$$X^{\bar{3}} = -X_C^{\bar{3}},$$
$$X^6 = X_C^6. \quad (21)$$

We can rewrite the effective Hamiltonian after a color Fierz transformation as

$$\mathcal{H}_{\mathrm{NPF}}^d = X^i \bar{d}_\beta \gamma_\mu (1+\gamma^5) b_\alpha \bar{s}_\alpha \gamma^\mu (1+\gamma^5) d_\beta$$
$$+ X_C^i \bar{d}_\beta \gamma_\mu (1+\gamma^5) b_\beta \bar{s}_\alpha \gamma^\mu (1-\gamma^5) d_\alpha. \quad (22)$$

The only other unsuppressed transition is $b \to s\bar{s}d$ ($b \to \bar{s}sd$ and $b \to \bar{s}ds$) which has the effective Hamiltonian,

$$\mathcal{H}_{\mathrm{NP}}^d = X^d \bar{s}_\alpha \gamma_\mu (1+\gamma^5) b_\alpha \bar{d}_\beta \gamma^\mu (1+\gamma^5) s_\beta$$
$$+ X_C^d \bar{s}_\alpha \gamma_\mu (1+\gamma^5) b_\beta \bar{d}_\beta \gamma^\mu (1+\gamma^5) s_\alpha, \quad (23)$$

with

$$X^d = -\frac{Y_{23}^d Y_{12}^{*d}}{4m_S^2},$$

$$X_C^d = -\frac{Y_{23}^d Y_{21}^{*d}}{4m_S^2}. \quad (24)$$

In this case at the meson level we can have the decays $B \to \phi\pi$ and the annihilation decays $B \to \phi\phi$. These decays are highly suppressed in the SM and the observance of these decays could signal the presence of diquarks.

TABLE I. Branching ratios, direct CP asymmetries A_{CP}, and mixing-induced CP asymmetry S_{CP} (if applicable) for the four $B \to \pi K$ decay modes. The data are taken from Ref. [52].

Mode	BR[10^{-6}]	A_{CP}	S_{CP}
$B^+ \to \pi^+ K^0$	23.79 ± 0.75	-0.017 ± 0.016	
$B^+ \to \pi^0 K^+$	12.94 ± 0.52	0.040 ± 0.021	
$B^0 \to \pi^- K^+$	19.57 ± 0.53	-0.082 ± 0.006	
$B^0 \to \pi^0 K^0$	9.93 ± 0.49	-0.01 ± 0.10	0.57 ± 0.17

B. Naive $B \to \pi K$ puzzle

We begin by reviewing the $B \to \pi K$ puzzle. As in Ref. [41] we can analyze the $B \to \pi K$ decays in terms of topological amplitudes. Including only the leading diagrams the $B \to \pi K$ amplitudes become

$$A^{+0} = -P_{tc}',$$
$$\sqrt{2}A^{0+} = -T'e^{i\gamma} + P_{tc}' - P_{\mathrm{EW}}',$$
$$A^{-+} = -T'e^{i\gamma} + P_{tc}',$$
$$\sqrt{2}A^{00} = -P_{tc}' - P_{\mathrm{EW}}'. \quad (25)$$

Here, T' is the color-allowed tree amplitude, P_{tc}' is the gluonic penguin amplitude, and P_{EW}' is the color-allowed electroweak penguin amplitude. Furthermore in the SU(3) limit the T' and P_{EW}' are proportional to each other and so have the same strong phases. Now consider the direct CP asymmetries of $B^+ \to \pi^0 K^+$ and $B^0 \to \pi^- K^+$. Such CP asymmetries are generated by the interference of two amplitudes with nonzero relative weak and strong phases. In both A^{0+} and A^{-+}, $T'-P_{tc}'$ interference leads to a direct CP asymmetry. On the other hand, in A^{0+}, P_{EW}' and T' have the same strong phase, $P_{\mathrm{EW}}' \propto T'$, while P_{EW}' and P_{tc}' have the same weak phase ($= 0$), so that P_{EW}' does not contribute to the direct CP asymmetry. This means that we expect $A_{CP}(B^+ \to \pi^0 K^+) = A_{CP}(B^0 \to \pi^- K^+)$.

The latest $B \to \pi K$ measurements are shown in Table I. Not only are $A_{CP}(B^+ \to \pi^0 K^+)$ and $A_{CP}(B^0 \to \pi^- K^+)$ not equal, they are of opposite sign! Experimentally, we have $(\Delta A_{CP})_{\mathrm{exp}} = (12.2 \pm 2.2)\%$. This differs from 0 by 5.5σ. This is the naive $B \to \pi K$ puzzle.

C. Model-independent new physics formalism

In the general approach of Refs. [53,54], the NP operators that contribute to the $B \to \pi K$ amplitudes take the form $\mathcal{O}_{\mathrm{NP}}^{ij,q} \sim \bar{s}\Gamma_i b\bar{q}\Gamma_j q$ ($q = u, d$), where $\Gamma_{i,j}$ represents Lorentz structures, and color indices are suppressed. The NP contributions to $B \to \pi K$ are encoded in the matrix elements $\langle \pi K | \mathcal{O}_{\mathrm{NP}}^{ij,q} | B \rangle$. In general, each matrix element has its own NP weak and strong phases.

Note that the strong phases are basically generated by QCD rescattering from diagrams with the same CKM

matrix elements. One can argue that the strong phase of T' is expected to be very small since it is due to self-rescattering. For the same reason, all NP strong phases are also small, and can be neglected. In this case, many NP matrix elements can be combined into a single NP amplitude, with a single weak phase:

$$\sum \langle \pi K | \mathcal{O}_{\mathrm{NP}}^{ij,q} | B \rangle = \mathcal{A}^q e^{i\Phi_q}. \tag{26}$$

Here the strong phase is zero. There are two classes of such NP amplitudes, differing only in their color structure: $\bar{s}_\alpha \Gamma_i b_\alpha \bar{q}_\beta \Gamma_j q_\beta$ and $\bar{s}_\alpha \Gamma_i b_\beta \bar{q}_\beta \Gamma_j q_\alpha$ ($q = u,\ d$). They are denoted $\mathcal{A}'^{,q} e^{i\Phi'_q}$ and $\mathcal{A}'^{C,q} e^{i\Phi'^C_q}$, respectively [54]. Here, Φ'_q and Φ'^C_q are the NP weak phases. In general, $\mathcal{A}'^{,q} \neq \mathcal{A}'^{C,q}$ and $\Phi'_q \neq \Phi'^C_q$. Note that, despite the "color-suppressed" index C, the matrix elements $\mathcal{A}'^{C,q} e^{i\Phi'^C_q}$ are not necessarily smaller than $\mathcal{A}'^{,q} e^{i\Phi'_q}$.

There are therefore four NP matrix elements that contribute to $B \to \pi K$ decays. However, only three combinations appear in the amplitudes: $\mathcal{A}'^{,\mathrm{comb}} e^{i\Phi'} \equiv -\mathcal{A}'^{,u} e^{i\Phi'_u} + \mathcal{A}'^{,d} e^{i\Phi'_d}$, $\mathcal{A}'^{C,u} e^{i\Phi'^C_u}$, and $\mathcal{A}'^{C,d} e^{i\Phi'^C_d}$ [54]. The $B \to \pi K$ amplitudes can now be written in terms of the SM diagrams and these NP matrix elements. Here we neglect the small SM diagram P'_{uc} but include the color-suppressed amplitudes:

$$A^{+0} = -P'_{tc} - \frac{1}{3} P'^C_{\mathrm{EW}} + \mathcal{A}'^{C,d} e^{i\Phi'^C_d},$$

$$\sqrt{2} A^{0+} = P'_{tc} - T' e^{i\gamma} - P'_{\mathrm{EW}} - C' e^{i\gamma} - \frac{2}{3} P'^C_{\mathrm{EW}} + \mathcal{A}'^{,\mathrm{comb}} e^{i\Phi'} - \mathcal{A}'^{C,u} e^{i\Phi'^C_u},$$

$$A^{-+} = P'_{tc} - T' e^{i\gamma} - \frac{2}{3} P'^C_{\mathrm{EW}} - \mathcal{A}'^{C,u} e^{i\Phi'^C_u},$$

$$\sqrt{2} A^{00} = -P'_{tc} - P'_{\mathrm{EW}} - C' e^{i\gamma} - \frac{1}{3} P'^C_{\mathrm{EW}} + \mathcal{A}'^{,\mathrm{comb}} e^{i\Phi'} + \mathcal{A}'^{C,d} e^{i\Phi'^C_d}. \tag{27}$$

We can express the various matrix elements as

$$\mathcal{A}'^{C,d} e^{i\Phi'^C_d} = \sqrt{2} \langle \pi^0 K^0 | \mathcal{H}_{\mathrm{NPF}}^d | B^0 \rangle = \langle \pi^+ K^0 | \mathcal{H}_{\mathrm{NPF}}^d | B^+ \rangle,$$

$$\mathcal{A}'^{C,u} e^{i\Phi'^C_u} = -\sqrt{2} \langle \pi^0 K^+ | \mathcal{H}_{\mathrm{NPF}}^u | B^+ \rangle = \langle \pi^- K^+ | \mathcal{H}_{\mathrm{NPF}}^u | B^0 \rangle,$$

$$\mathcal{A}'^{,\mathrm{comb}} e^{i\Phi'} = \sqrt{2} \langle \pi^0 K^+ | [\mathcal{H}_{\mathrm{NP}}^u + \mathcal{H}_{\mathrm{NP}}^d] | B^+ \rangle$$
$$= \sqrt{2} \langle \pi^0 K^0 | [\mathcal{H}_{\mathrm{NP}}^u + \mathcal{H}_{\mathrm{NP}}^d] | B^0 \rangle. \tag{28}$$

In our model $\mathcal{H}_{\mathrm{NP}}^u$ and $\mathcal{H}_{\mathrm{NPF}}^u$ are absent while $\mathcal{H}_{\mathrm{NP}}^d$ and $\mathcal{H}_{\mathrm{NPF}}^d$ are defined in Eqs. (19) and (22). In the factorization assumption and using Eqs. (19) and (22) we get the following results for the nonzero amplitudes:

$$\mathcal{A}'^{C,d} e^{i\Phi'^C_d} = \left[X^6 - X^{\bar{3}} + \frac{X^6 + X^{\bar{3}}}{N_c} \right] \langle \pi^+ | \bar{d}_\beta \gamma_\mu (1 + \gamma^5) b_\beta | B^+ \rangle$$
$$\times \langle K^0 | \bar{s}_\alpha \gamma^\mu (1 + \gamma^5) d_\alpha | 0 \rangle,$$

$$\mathcal{A}'^{,d} e^{i\Phi'_d} = \sqrt{2} \left[X^6 + X^{\bar{3}} + \frac{X^6 - X^{\bar{3}}}{N_c} \right]$$
$$\times \langle K^+ | \bar{s}_\beta \gamma_\mu (1 + \gamma^5) b_\beta | B^+ \rangle$$
$$\times \langle \pi^0 | \bar{d}_\alpha \gamma^\mu (1 + \gamma^5) d_\alpha | 0 \rangle. \tag{29}$$

In Ref. [55], a different set of NP operators is defined:

$$P'_{\mathrm{EW,NP}} e^{i\Phi'_{\mathrm{EW}}} \equiv \mathcal{A}'^{,u} e^{i\Phi'_u} - \mathcal{A}'^{,d} e^{i\Phi'_d},$$

$$P'_{\mathrm{NP}} e^{i\Phi'_P} \equiv \frac{1}{3} \mathcal{A}'^{C,u} e^{i\Phi'^C_u} + \frac{2}{3} \mathcal{A}'^{C,d} e^{i\Phi'^C_d},$$

$$P'^C_{\mathrm{EW,NP}} e^{i\Phi'^C_{\mathrm{EW}}} \equiv \mathcal{A}'^{C,u} e^{i\Phi'^C_u} - \mathcal{A}'^{C,d} e^{i\Phi'^C_d}. \tag{30}$$

In this case we have

$$P'_{\mathrm{EW,NP}} e^{i\Phi'_{\mathrm{EW}}} \equiv -\mathcal{A}'^{,d} e^{i\Phi'_d},$$

$$P'_{\mathrm{NP}} e^{i\Phi'_P} \equiv \frac{2}{3} \mathcal{A}'^{C,d} e^{i\Phi'^C_d} = -(2/3) P'^C_{\mathrm{EW,NP}}$$

$$P'^C_{\mathrm{EW,NP}} e^{i\Phi'^C_{\mathrm{EW}}} \equiv -\mathcal{A}'^{C,d} e^{i\Phi'^C_d}. \tag{31}$$

We consider two models, the first with

$$X^6 = X^{\bar{3}}. \tag{32}$$

This leads to $P'^C_{\mathrm{EW,NP}} / P'_{\mathrm{EW,NP}} = \frac{1}{3}$ with both amplitudes having the same weak phase,

$$P'_{\mathrm{EW,NP}} e^{i\Phi'_{\mathrm{EW}}} \equiv \frac{Y^6_{d13} Y^{*6}_{d12}}{4 m_S^2} \sqrt{2} \langle K^+ | \bar{s}_\beta \gamma_\mu (1 + \gamma^5) b_\beta | B^+ \rangle$$
$$\times \langle 0 | \bar{s}_\alpha \gamma^\mu (1 + \gamma^5) d_\alpha | K^0 \rangle,$$

$$P'_{\mathrm{NP}} e^{i\Phi'_P} \equiv \frac{2}{3} \mathcal{A}'^{C,d} e^{i\Phi'^C_d} = -(2/3) P'^C_{\mathrm{EW,NP}},$$

$$P'^C_{\mathrm{EW,NP}} e^{i\Phi'^C_{\mathrm{EW}}} \equiv -\mathcal{A}'^{C,d} e^{i\Phi'^C_d} = P'_{\mathrm{EW,NP}} e^{i\Phi'_{\mathrm{EW}}} / 3. \tag{33}$$

The second model has

$$X^{\bar{3}} = 0. \tag{34}$$

This leads to $P'^C_{\mathrm{EW,NP}} / P'_{\mathrm{EW,NP}} = 1$, again with both amplitudes having the same weak phase.

A χ^2 fit for the new physics within this scenario is performed to determine the parameters of the model. The procedure for determining such a fit is as follows. We define the function

TABLE II. $\chi^2_{\min}/$d.o.f. and best-fit values of unknown parameters for the Diquark model where the fit 1 has $X^6 = X^{\bar{3}}$. Constraints: $B \to \pi K$ data, measurements of β and γ, $|C'/T'| = 0.2$, $|P'^C_{EW,NP}/P'_{EW,NP}| = 0.3$.

NP fit (1): $\chi^2/$d.o.f. $= 3.75/4$, p value $= 0.44$	
Parameter	Best-fit value
γ	$(67.5 \pm 3.4)°$
β	$(21.80 \pm 0.68)°$
Φ'	$(37.0 \pm 12.6)°$
$|T'|$	19.1 ± 2.8
$|P'_{tc}|$	48.7 ± 1.2
$P'_{EW,NP}$	8.6 ± 2.5
$P'^C_{EW,NP}$	2.7 ± 1.1
$\delta_{P'_{tc}}$	$(-4.0 \pm 1.1)°$
$\delta_{C'}$	$(-60.0 \pm 115.6)°$

$$\chi^2 = \sum_{i=1}^{N} \left(\frac{\mathcal{O}_{\exp} - \mathcal{O}_{th}}{\Delta\mathcal{O}_{\exp}} \right)^2 \tag{35}$$

where $\mathcal{O}_{\exp}$ and $\Delta\mathcal{O}_{\exp}$ are the experimentally determined quantities with their associated uncertainties, respectively, as listed in Table I. $\mathcal{O}_{th}$ are determined from the model and are thus functions of the unknown parameters. The goal from here is to find the values of the parameters that minimize χ^2. There are many programs available to accomplish this, one of the most widely used is MINUIT [56], which is used here. The goodness of the fit is determined by the value of χ^2 at the minimum and the number of degrees of freedom (d.o.f.) in the fit. The d.o.f. are the number of constraints included in the fit minus the number of parameters that are fitted. In this case the number of constraints is 13: the $B \to \pi K$ data, the independent measurements of β and γ, and the constraints on $|C'/T'|$ and $|P'^C_{EW,NP}/P'_{EW,NP}|$. The number of parameters is nine and we have that the number of d.o.f. are four. A "good" fit is one where $\chi^2_{\min} \approx$ d.o.f., but a better measure is the p value which gives the probability that the model tested adequately describes the observations.

The results of the fit for this case are shown in Tables II and III. Here the p value is 44% for $X^6 = X^{\bar{3}}$, and 43% for $X^{\bar{3}} = 0$, which is not bad (and is far better than that of the SM).

The SM T' diagram involves the tree-level decay $\bar{b} \to \bar{u}W^{+*}(\to u\bar{s} = K^+)$. The NP $P'_{EW,NP}$ diagram looks very similar and is expressed relative to the T' diagram. Within factorization, the SM and NP diagrams involve $A_{\pi K} \equiv F_0^{B\to\pi}(0)f_K$ and $A_{K\pi} \equiv F_0^{B\to K}(0)f_\pi$, respectively, where $F_0^{B\to K,\pi}(0)$ are form factors and $f_{\pi,K}$ are decay constants. The hadronic factors are similar in size: $|A_{K\pi}/A_{\pi K}| = 0.9 \pm 0.1$ [44]. Taking central values for $X^6 = X^{\bar{3}}$, we have [41]
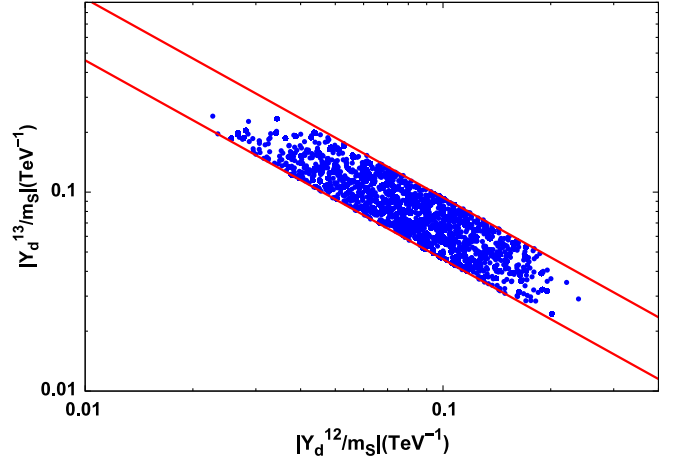

FIG. 2. The correlation between $\frac{|Y_d^{12}|}{m_S}$ and $\frac{|Y_d^{13}|}{m_S}$ within 1σ range. The shaded area corresponds to mass range $m_S \in [5:20]$ TeV.

$$\Phi' = \mathrm{Arg}[Y_{d13}^6 Y_{d12}^{*6}]$$

$$\left| \frac{P'_{EW,NP}}{T'} \right| \simeq \frac{2A_{K\pi}|X^{\bar{3}}|}{A_{\pi K}(G_F/\sqrt{2})|V_{ub*}V_{us}|} = \frac{8.6}{19.1}$$

$$\Rightarrow \left| \frac{Y_{d13}^6 Y_{d12}^{*6}}{2m_S^2} \right| = (3.4 \pm 1.2) \times 10^{-3} \text{ TeV}^{-2}. \tag{36}$$

For $X^{\bar{3}} = 0$ we obtain

$$\left| \frac{Y_{d13}^6 Y_{d12}^{*6}}{2m_S^2} \right| = (2.6 \pm 1.8) \times 10^{-3} \text{ TeV}^{-2}. \tag{37}$$

Both models give similar fits and in Fig. 2 we show the allowed regions of the diquark couplings within a 1σ range for the first model.

D. Neutral meson mixing

Diquarks, in spite of being charged, through their coupling to the same generation quarks can mediate the mixing between neutral mesons at tree level. Following the convention in [57], the mixing can be depicted as the six dimension operator:

$$\mathcal{O}_{mix} = \frac{Y_d^{*ij} Y_d^{kl}}{m_S^2} \bar{\psi}^k_R \gamma^\mu \psi^i_R \bar{\psi}^l_R \gamma_\mu \psi^j_R.$$

The 90% C.L. bounds on the corresponding Wilson coefficients [57] is then given as

$$\mathbf{K^\circ - \overline{K^\circ}} \quad \left| \frac{Y_d^{*11} Y_d^{22}}{4\sqrt{2}G_F m_S^2} \right| < 2.9 \times 10^{-8},$$

$$\mathbf{B_d^\circ - \overline{B_d^\circ}} \quad \left| \frac{Y_d^{*11} Y_d^{33}}{4\sqrt{2}G_F m_S^2} \right| < 7.0 \times 10^{-7},$$

$$\mathbf{B_s^\circ - \overline{B_s^\circ}} \quad \left| \frac{Y_d^{*22} Y_d^{33}}{4\sqrt{2}G_F m_S^2} \right| < 3.3 \times 10^{-5}.$$

V. NUMERICAL ANALYSIS AND DISCUSSION

Before we present the results, we discuss the bounds on the scalar masses obtained from collider experiments. The collider experiments provide direct limits on the leptoquark mass when they decay to leptons and quarks in the final state. There are many studies in the literature where different signatures have been discussed [32,58,59]. The leptoquarks can be pair produced from gg and $q\bar{q}$ as initial state or singly produced at hadron colliders via $g + q \rightarrow S_{3L} +$ lepton. Recent studies at ATLAS [60] and CMS [61] with 13 TeV data puts a bound on the scalar leptoquark mass, $m_L > 1, 1.2$ (ATLAS), 0.9 (CMS) TeV when decay to ue, $c\mu$, and $t\tau$ with 100% branching fraction, respectively, at 95% C.L. The previous results [62,63] at 8 TeV from the search of single leptoquark production are of order 0.65 TeV for final state $c\mu$. Taking a cue from these studies, we take $m_L > 1.5$ TeV in our analysis.

Similar to the leptoquarks, diquarks can be looked at the LHC through dijets in the final state. The recent studies at CMS on dijets' final states rules out scalar diquarks of mass smaller than 6 TeV. However, these limits are derived for E_6 diquark which couples with an up-type quark and a down-type quark [64]. These limits are very sensitive to the assumptions of decay branching fractions as well as the flavor dependent coupling strengths. Also, the diquark in the present work couples only to down-type quarks. This leads to a decrease in the flux factor and hence the cross section and thereby the bounds on m_S would be lower. Hence, we take $m_S \in [5:20]$ TeV in our analysis.

With this mass range of scalars, we randomly generate a sample of diquark couplings satisfying the constraints discussed in Sec. III. For $m_S \in [5:20]$ TeV, the $B \rightarrow \pi K$ fit requires $Y_d^{12,13}$ to be greater than 0.1. Thus, we generate these couplings randomly in the range $[0.1:1]$. We fix Y_d^{23} of the order 10^{-2} and Y_d^{33} is randomly generated in the range $[10^{-4}:10^{-2}]$. The small value of Y_d^{33} is required to generate a small neutrino mass because the Y_d^{33} coupling is always multiplied to the square of a bottom quark mass when mass matrix, in Eq. (4), is solved. For the remaining Y_d^{ij}, i.e., $Y_d^{11,12}$, we scan in the range $[10^{-5}:1]$. Except for Y_d^{23}, other diquark couplings are assumed complex. It should be noted that the signs of the couplings are randomly assigned with equal probabilities being positive or negative in the whole calculation.
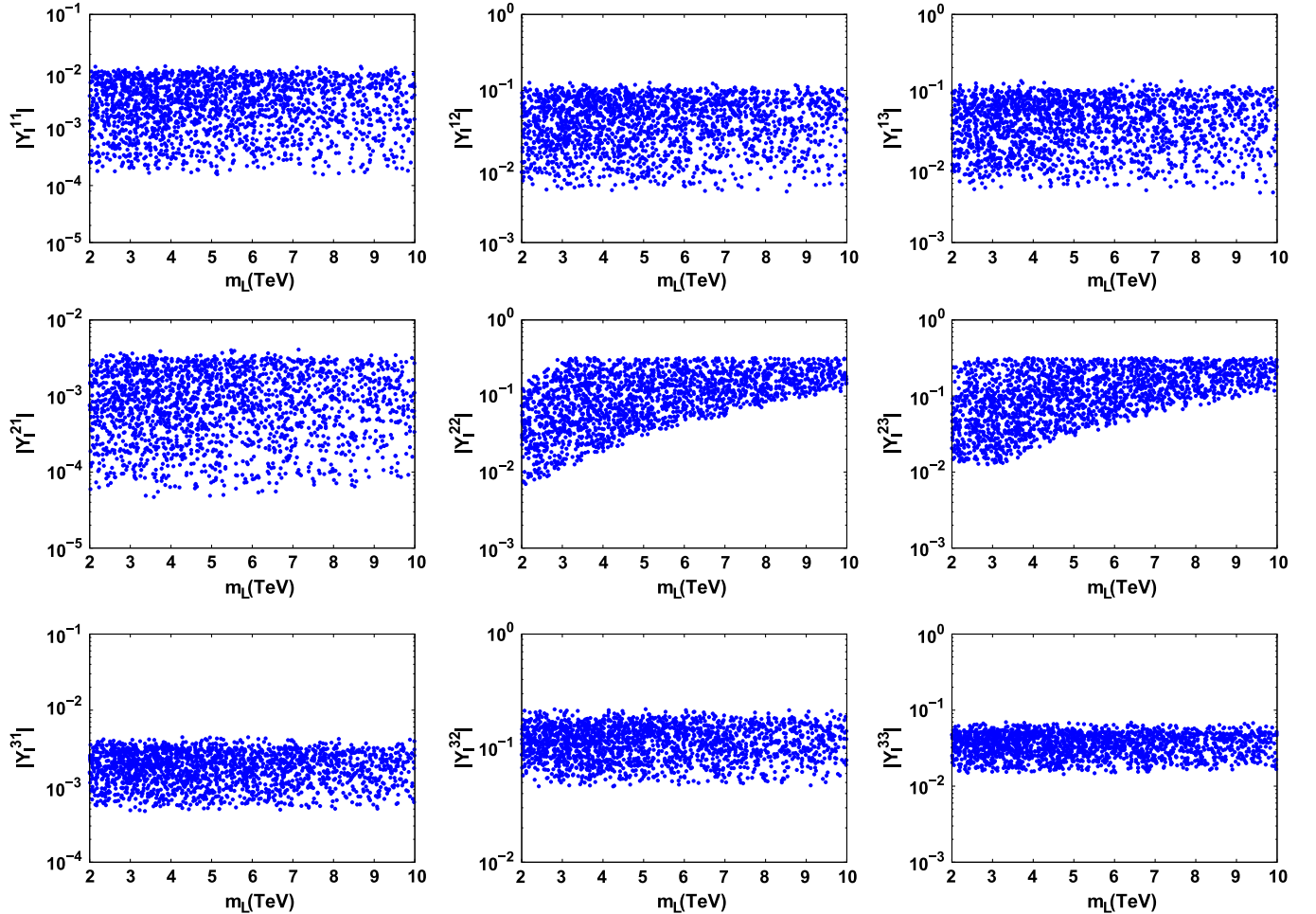

FIG. 3.   Parameter space scan in Y_l^{ij}-m_L plane.

As for the leptoquark case, Y_l^{2i} couplings (real) are generated randomly in the range $[10^{-5}:1]$. With the obtained sets of couplings, we calculate the strength of remaining leptoquark couplings, for randomly generated LQ mass, from Eq. (4) to get the correct neutrino masses. The symmetric neutrino mass matrix in Eq. (4) represents six independent equations as six independent parameters (given in Table IV) that are obtained from the neutrino oscillation experiments. Throughout the analysis, we have kept Majorana phases to be 0, and have employed the 2σ ranges for the neutrino mixing parameters for normal hierarchy from Refs. [65,66]. Finally, those sets of LQ couplings are selected that satisfy all of the constraints in Sec. III. The results for the LQ couplings are given in Fig. 3.

The pattern in the lower limit of the $Y_l^{22,23}$ coupling is mainly decided by $b \to s\ell^+\ell^-$ anomalies whereas the DQ couplings, $Y_d^{12/13}$, do not contribute significantly to neutrino mass calculations and thereby leptoquark parameter space as $Y_d^{12/13}$ comes with the product of down and strange/bottom quark masses in Eq. (4), and the down quark mass is very small.

We compare our results for leptoquark coupling with the results given in [33,67] and find them consistent. A few benchmark points (BP) are given in the Appendix B. For these BP, we present branching ratios for the rare decays in Table V following the calculations in Ref. [51]. The branching ratios are rather small and it will be difficult to observe these decays in ongoing experiments. Our analysis shows that the B anomalies and the neutrino masses can all be accommodated in a consistent framework.

VI. CONCLUSION

In conclusion we have discussed a unified framework to provide solutions to three problems. They are the anomalies in $b \to s\mu^+\mu^-$ measurements, nonleptonic $B \to \pi K$ decays, and the issue of generating neutrino masses and mixing. Our framework contained a scalar triplet leptoquark, a scalar color sextext diquark, and also, possibly, a color antitriplet diquark. We considered several low energy as well as collider bounds on the leptoquark, diquark couplings, and masses. For the leptoquarks these low energy observables included the $b \to s\ell^+\ell^-$ measurements. The solutions to the $B \to \pi K$ puzzle provided constraints on products of the diquark Yukawa couplings. We then checked that the correct neutrino masses and mixings were reproduced with the allowed couplings of the leptoquarks and diquarks. We also predicted the branching ratios for a few rare B decays whose observations could signal the existence of diquarks. However, we found the branching ratios of these decays to be unobservably small.

ACKNOWLEDGMENTS

APPENDIX A: SOME USEFUL EXPRESSIONS

In this Appendix, we give some useful expressions and calculations that could be useful while reading the paper

$$\psi^c = C\bar{\psi}^T,$$
$$\bar{\psi}^c = (\psi^c)^\dagger \gamma^0 = -\psi^T C^{-1},$$
$$(\gamma^\mu)^T = -C^{-1}\gamma^\mu C,$$
$$C^{-1} = C^\dagger, \tag{A1}$$

$$H = Y_d^{ij} \bar{d}_{i\alpha}^c P_R d_{j\beta} S^{\alpha\beta},$$
$$H^\dagger = Y_d^{ij*} d_{j\beta}^\dagger P_R (-d_{i\alpha}^T C^{-1})^\dagger S^{*\alpha\beta}$$
$$= -Y_d^{ij*} \bar{d}_{j\beta} P_L (\gamma^0 C d_{i\alpha}^*) S^{*\alpha\beta}. \tag{A2}$$

Integrating out diquark

$$H_{\text{eff}} = -Y_d^{13} \bar{d}_\alpha^c P_R b_\beta S^{\alpha\beta} \otimes Y_d^{12*} s_\beta^\dagger P_R (-d_\alpha^T C^{-1})^\dagger S^{*\alpha\beta}$$
$$= -\frac{Y_d^{13} Y_d^{12*}}{m_S^2} \bar{d}_\alpha^c P_R b_\beta \bar{s}_\beta P_L (\gamma^0 C d_\alpha^*)$$
$$= \frac{Y_d^{13} Y_d^{12*}}{2m_S^2} \bar{d}_\alpha^c \gamma^\mu P_L (\gamma^0 C d_\alpha^*) \bar{s}_\beta \gamma_\mu P_R b_\beta$$
$$= \frac{Y_d^{13} Y_d^{12*}}{2m_S^2} \bar{s}_\beta \gamma_\mu P_R b_\beta [-d_\alpha^T C^{-1} \gamma^\mu P_L (\gamma^0 C d_\alpha^*)]$$
$$= -\frac{Y_d^{13} Y_d^{12*}}{2m_S^2} \bar{s}_\beta \gamma_\mu P_R b_\beta [d_\alpha^T \gamma^{\mu T} P_L^T (\gamma^{0T} d_\alpha^*)]$$
$$= -\frac{Y_d^{13} Y_d^{12*}}{2m_S^2} \bar{s}_\beta \gamma_\mu P_R b_\beta [d_\alpha^\dagger \gamma^0 P_L \gamma^\mu d_\alpha]^T$$
$$= \frac{Y_d^{13} Y_d^{12*}}{2m_S^2} \bar{s}_\beta \gamma_\mu P_R b_\beta \overline{d_\alpha} \gamma^\mu P_R d_\alpha. \tag{A3}$$

TABLE III. χ^2_{min}/d.o.f. and best-fit values of unknown parameters for the Diquark model where the fit 2 has $X^{\bar{3}} = 0$. Constraints: $B \to \pi K$ data, measurements of β and γ, and $|P'^C_{\text{EW,NP}}/P'_{\text{EW,NP}}| = 1$.

NP fit (2): χ^2/d.o.f. $= 3.82/4$, p value $= 0.43$

Parameter	Best-fit value
γ	$(74.7 \pm 5.2)°$
β	$(21.80 \pm 0.68)°$
Φ'	$(18.7 \pm 33.9)°$
$|T'|$	19.7 ± 7.1
$|P'_{tc}|$	45.5 ± 3.9
$P'_{\text{EW,NP}}$	6.7 ± 3.9
$P'^C_{\text{EW,NP}}$	6.5 ± 3.7
$\delta_{P'_{tc}}$	$(-4.0 \pm 2.0)°$
$\delta_{C'}$	$(-48.9 \pm 23.5)°$

TABLE IV. Neutrino data with 2σ deviation for normal hierarchy [65,66].

δm^2	$7.07 - 7.73 \times 10^{-5}$ eV^2
$\sin^2\theta_{12}$	0.265–0.334
$|\Delta m^2|$	$2.454 - 2.606 \times 10^{-3}$ eV^2
$\sin^2\theta_{13}$	0.0199–0.0231
$\sin^2\theta_{23}$	0.395–0.470
δ/π	1.00–1.90

TABLE V. Branching ratios obtained with the couplings that can produce required neutrino mass and also satisfy the constraints coming from the $B \to \pi K$ puzzle.

B.P	BR($B^\pm \to \phi\pi^\pm$)	BR($B^0 \to \phi\pi^\circ$)	BR($B^0 \to \phi\phi$)
A	1.45×10^{-10}	7.2×10^{-11}	1.45×10^{-12}
B	6.5×10^{-14}	3.2×10^{-14}	6.5×10^{-16}
C	1.19×10^{-12}	5.95×10^{-13}	1.19×10^{-14}

Because $S^{\alpha\beta}$ is symmetric/antisymmetric there is an additional factor of 2. In other words S^{12} can contract with S^{12} and S^{21}.

APPENDIX B: BENCHMARK POINTS

Here we give the benchmark points satisfying the B anomalies observations and explaining the neutrino mass.

(i) BP A:

$$m_L = 3.5 \text{ TeV}, \quad m_S = 5 \text{ TeV}$$

$$Y_l = \begin{pmatrix} 1.40 \times 10^{-4} + i3.24 \times 10^{-4} & 5.02 \times 10^{-3} + i8.9 \times 10^{-3} & 3.7 \times 10^{-3} + i3.26 \times 10^{-2} \\ 1.37 \times 10^{-3} + i2.83 \times 10^{-4} & 1.81 \times 10^{-1} & 2.44 \times 10^{-2} \\ 5.03 \times 10^{-4} + i3.12 \times 10^{-3} & 1.4 \times 10^{-1} + i3.31 \times 10^{-2} & 1.1 \times 10^{-2} + i4.5 \times 10^{-2} \end{pmatrix}. \quad \text{(B1)}$$

$$Y_d = \begin{pmatrix} 1.68 \times 10^{-4} & 4.6 \times 10^{-1} + i1.22 \times 10^{-1} & 4.64 \times 10^{-1} + i1.3 \times 10^{-2} \\ 4.6 \times 10^{-1} + i1.22 \times 10^{-1} & 2 \times 10^{-1} & 0.01 \\ 4.64 \times 10^{-1} + i1.3 \times 10^{-2} & 0.01 & -1.42 \times 10^{-4} + i2.5 \times 10^{-4} \end{pmatrix}.$$

$$(M_\nu)_{ee} = 4.53 \times 10^{-3} \text{ eV} \quad \text{(B2)}$$

(ii) BP B:

$$m_L = 7.5 \text{ TeV}, \quad m_S = 6 \text{ TeV}$$

$$Y_l = \begin{pmatrix} 1.03 \times 10^{-4} + i7.8 \times 10^{-3} & 8.2 \times 10^{-3} + i1.2 \times 10^{-2} & 1.87 \times 10^{-2} + i1.11 \times 10^{-2} \\ 1.32 \times 10^{-3} + i3.2 \times 10^{-4} & 2.15 \times 10^{-1} & 9.5 \times 10^{-2} \\ 7.56 \times 10^{-4} + i1.91 \times 10^{-3} & 1.23 \times 10^{-1} + i1.25 \times 10^{-1} & 3.2 \times 10^{-2} + i1.51 \times 10^{-2} \end{pmatrix}. \quad \text{(B3)}$$

$$Y_d = \begin{pmatrix} 1.38 \times 10^{-4} & 6.28 \times 10^{-2} + i3.6 \times 10^{-1} & 5.1 \times 10^{-1} + i2.12 \times 10^{-2} \\ 6.28 \times 10^{-2} + i3.6 \times 10^{-1} & 1.8 \times 10^{-1} & 0.01 \\ 5.1 \times 10^{-1} + i2.12 \times 10^{-2} & 0.01 & -1.4 \times 10^{-3} + i3 \times 10^{-4} \end{pmatrix}.$$

$$(M_\nu)_{ee} = 1.55 \times 10^{-3} \text{ eV} \quad \text{(B4)}$$

(iii) BP C:

$$m_L = 5.0 \text{ TeV}, \quad m_S = 7.5 \text{ TeV}$$

$$Y_l = \begin{pmatrix} 5.1 \times 10^{-3} + i2.63 \times 10^{-4} & 4.6 \times 10^{-2} + i5.2 \times 10^{-2} & 3.3 \times 10^{-3} + i1.1 \times 10^{-2} \\ 7.26 \times 10^{-4} + i1.55 \times 10^{-3} & 2.42 \times 10^{-1} & 4.3 \times 10^{-2} \\ 1.57 \times 10^{-3} + i1.64 \times 10^{-3} & 1.24 \times 10^{-1} + i1.06 \times 10^{-1} & 1.32 \times 10^{-2} + i1.0 \times 10^{-2} \end{pmatrix}. \quad \text{(B5)}$$

$$Y_d = \begin{pmatrix} 1.2 \times 10^{-4} & 3.04 \times 10^{-1} + i7.3 \times 10^{-1} & 5.1 \times 10^{-1} + i1.79 \times 10^{-1} \\ 3.04 \times 10^{-1} + i7.3 \times 10^{-1} & 7.2 \times 10^{-1} & 0.01 \\ 5.1 \times 10^{-1} + i1.79 \times 10^{-1} & 0.01 & -1.43 \times 10^{-2} - i5.11 \times 10^{-3} \end{pmatrix}.$$

$$(M_\nu)_{ee} = 1.01 \times 10^{-3} \text{ eV} \quad \text{(B6)}$$

 [1] B. Bhattacharya, A. Datta, D. London, and S. Shivashankara, Phys. Lett. B **742**, 370 (2015).
 [2] A. K. Alok, A. Datta, A. Dighe, M. Duraisamy, D. Ghosh, and D. London, J. High Energy Phys. 11 (2011) 121.
 [3] A. K. Alok, A. Datta, A. Dighe, M. Duraisamy, D. Ghosh, and D. London, J. High Energy Phys. 11 (2011) 122.
 [4] R. Aaij et al. (LHCb Collaboration), Phys. Rev. Lett. **111**, 191801 (2013).
 [5] R. Aaij et al. (LHCb Collaboration), J. High Energy Phys. 02 (2016) 104.
 [6] A. Abdesselam et al. (Belle Collaboration), arXiv:1604.04042.
 [7] The ATLAS Collaboration, Report No. ATLAS-CONF-2017-023, 2017.
 [8] CMS Collaboration, Report No. CMS-PAS-BPH-15-008, 2017.
 [9] R. Aaij et al. (LHCb Collaboration), J. High Energy Phys. 07 (2013) 084.
 [10] R. Aaij et al. (LHCb Collaboration), J. High Energy Phys. 09 (2015) 179.
 [11] R. Aaij et al. (LHCb Collaboration), Phys. Rev. Lett. **113**, 151601 (2014).
 [12] R. Aaij et al. (LHCb Collaboration), Phys. Rev. Lett. **122**, 191801 (2019).
 [13] R. Aaij et al. (LHCb Collaboration), J. High Energy Phys. 08 (2017) 055.
 [14] A. Abdesselam et al. (Belle Collaboration), arXiv:1904.02440.
 [15] A. Datta, M. Duraisamy, and D. Ghosh, Phys. Rev. D **89**, 071501 (2014).
 [16] A. Datta, J. Kumar, J. Liao, and D. Marfatia, Phys. Rev. D **97**, 115038 (2018).
 [17] A. Datta, J. Kumar, and D. London, arXiv:1903.10086.
 [18] A. K. Alok, A. Dighe, S. Gangal, and D. Kumar, J. High Energy Phys. 06 (2019) 089.
 [19] M. Ciuchini, A. M. Coutinho, M. Fedele, E. Franco, A. Paul, L. Silvestrini, and M. Valli, arXiv:1903.09632.
 [20] J. Aebischer, W. Altmannshofer, D. Guadagnoli, M. Reboud, P. Stangl, and D. M. Straub, arXiv:1903.10434.
 [21] M. Alguero, B. Capdevila, S. Descotes-Genon, P. Masjuan, and J. Matias, J. High Energy Phys. 07 (2019) 096.
 [22] K. Kowalska, D. Kumar, and E. M. Sessolo, arXiv:1903.10932.
 [23] L. Calibbi, A. Crivellin, and T. Ota, Phys. Rev. Lett. **115**, 181801 (2015).
 [24] B. Bhattacharya, A. Datta, J.-P. Guevin, D. London, and R. Watanabe, J. High Energy Phys. 01 (2017) 015.
 [25] A. Greljo, G. Isidori, and D. Marzocca, J. High Energy Phys. 07 (2015) 142.
 [26] J. Kumar, D. London, and R. Watanabe, Phys. Rev. D **99**, 015007 (2019).
 [27] A. Datta, J. Liao, and D. Marfatia, Phys. Lett. B **768**, 265 (2017).
 [28] A. K. Alok, B. Bhattacharya, A. Datta, D. Kumar, J. Kumar, and D. London, Phys. Rev. D **96**, 095009 (2017).
 [29] A. Datta, B. Dutta, S. Liao, D. Marfatia, and L. E. Strigari, J. High Energy Phys. 01 (2019) 091.
 [30] F. Sala and D. M. Straub, Phys. Lett. B **774**, 205 (2017).
 [31] W. Altmannshofer, M. J. Baker, S. Gori, R. Harnik, M. Pospelov, E. Stamou, and A. Thamm, J. High Energy Phys. 03 (2018) 188.
 [32] M. Kohda, H. Sugiyama, and K. Tsumura, Phys. Lett. B **718**, 1436 (2013).
 [33] S.-Y. Guo, Z.-L. Han, B. Li, Y. Liao, and X.-D. Ma, Nucl. Phys. **B928**, 435 (2018).
 [34] O. Popov and G. A. White, Nucl. Phys. **B923**, 324 (2017).
 [35] C. Marzo, L. Marzola, and M. Raidal, arXiv:1901.08290.
 [36] O. Cata and T. Mannel, arXiv:1903.01799.
 [37] A. J. Buras, R. Fleischer, S. Recksiegel, and F. Schwab, Eur. Phys. J. C **32**, 45 (2003).
 [38] A. J. Buras, R. Fleischer, S. Recksiegel, and F. Schwab, Phys. Rev. Lett. **92**, 101804 (2004).
 [39] A. J. Buras, R. Fleischer, S. Recksiegel, and F. Schwab, Nucl. Phys. **B697**, 133 (2004).
 [40] S. Baek, P. Hamel, D. London, A. Datta, and D. A. Suprun, Phys. Rev. D **71**, 057502 (2005).
 [41] N. B. Beaudry, A. Datta, D. London, A. Rashed, and J.-S. Roux, J. High Energy Phys. 01 (2018) 074.
 [42] R. Fleischer, R. Jaarsma, and K. K. Vos, Phys. Lett. B **785**, 525 (2018).
 [43] R. Fleischer, R. Jaarsma, E. Malami, and K. K. Vos, Eur. Phys. J. C **78**, 943 (2018).
 [44] M. Beneke, G. Buchalla, M. Neubert, and C. T. Sachrajda, Nucl. Phys. **B606**, 245 (2001).
 [45] K. S. Babu and C. N. Leung, Nucl. Phys. **B619**, 667 (2001).
 [46] K. Cheung, T. Nomura, and H. Okada, Phys. Rev. D **95**, 015026 (2017).
 [47] D. A. Sierra and M. Hirsch, J. High Energy Phys. 12 (2006) 052.
 [48] M. Carpentier and S. Davidson, Eur. Phys. J. C **70**, 1071 (2010).
 [49] A. M. Baldini et al. (MEG Collaboration), Eur. Phys. J. C **76**, 434 (2016).
 [50] B. Aubert et al. (BABAR Collaboration), Phys. Rev. Lett. **104**, 021802 (2010).
 [51] G. F. Giudice, B. Gripaios, and R. Sundrum, J. High Energy Phys. 08 (2011) 055.
 [52] Y. Amhis et al., Averages of b-hadron, c-hadron, and τ-lepton properties as of winter 2016, http://www.slac.stanford.edu/xorg/hfag/semi/winter16/winter16_dtaunu.html.
 [53] A. Datta and D. London, Phys. Lett. B **595**, 453 (2004).
 [54] A. Datta, M. Imbeault, D. London, V. Page, N. Sinha, and R. Sinha, Phys. Rev. D **71**, 096002 (2005).
 [55] S. Baek, C.-W. Chiang, and D. London, Phys. Lett. B **675**, 59 (2009).
 [56] F. James, Report No. CERN-D-506, CERN-D506, 1994.
 [57] M. Bona et al. (UTfit Collaboration), J. High Energy Phys. 03 (2008) 049.
 [58] G. Bhattacharyya, D. Choudhury, and K. Sridhar, Phys. Lett. B **349**, 118 (1995).
 [59] P. Bandyopadhyay and R. Mandal, Eur. Phys. J. C **78**, 491 (2018).

[60] M. Aaboud *et al.* (ATLAS Collaboration), New J. Phys. **18,** 093016 (2016).

[61] A. M. Sirunyan *et al.* (CMS Collaboration), Eur. Phys. J. C **78,** 707 (2018).

[62] V. Khachatryan *et al.* (CMS Collaboration), Phys. Rev. D **93,** 032004 (2016).

[63] V. Khachatryan *et al.* (CMS Collaboration), J. High Energy Phys. 07 (2015) 042; 11 (2016) 056.

[64] V. Khachatryan *et al.* (CMS Collaboration), Phys. Rev. Lett. **116,** 071801 (2016).

[65] F. Capozzi, E. Di Valentino, E. Lisi, A. Marrone, A. Melchiorri, and A. Palazzo, Phys. Rev. D **95,** 096014 (2017).

[66] M. Tanabashi *et al.* (Particle Data Group), Phys. Rev. D **98,** 030001 (2018).

[67] G. Hiller and I. Nisandzic, Phys. Rev. D **96,** 035003 (2017).